5-30-2023

Resting-state cortical hubs in youth organize into four categories

Damion V Demeter

Evan M Gordon

Tehila Nugiel

AnnaCarolina Garza

Tyler L Larguinho

See next page for additional authors

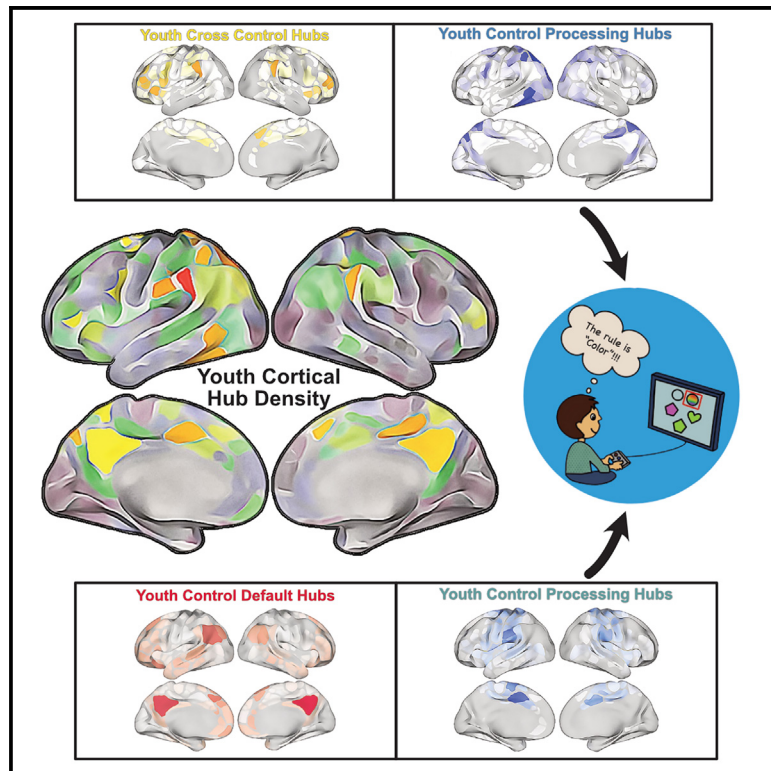## Authors

Damion V Demeter, Evan M Gordon, Tehila Nugiel, AnnaCarolina Garza, Tyler L Larguinho, and Jessica A Church

Resting-state cortical hubs in youth organize into four categories

Graphical abstract

Authors

Damion V. Demeter, Evan M. Gordon, Tehila Nugiel, AnnaCarolina Garza, Tyler L. Larguinho, Jessica A. Church

Correspondence

ddemeter@ucsd.edu

In brief

Cortical hubs integrate information flow between brain regions and are especially important as the brain undergoes rapid growth during childhood. Demeter et al. identify four unique categories of cortical hubs in youths. Notably, control-processing hubs split into two distinct and sensory-specific categories that are associated with cognitive flexibility task performance.

Highlights

- Youth cortical hubs exhibit strong cross-network coactivation

- Four distinct resting-state hub profile categories are established in childhood

- Youth control-processing hubs form two unique sensory-specific categories

- Control-processing hubs are related to youth cognitive flexibility task performance

CellPress

Article

Resting-state cortical hubs in youth organize into four categories

Damion V. Demeter,[1,5,*] Evan M. Gordon,[2] Tehila Nugiel,[3] AnnaCarolina Garza,[4] Tyler L. Larguinho,[4] and Jessica A. Church[4]

[1]Department of Cognitive Science, University of California San Diego, La Jolla, CA 92093, USA
[2]Department of Radiology, Washington University School of Medicine, St. Louis, MO 63110, USA
[3]Carolina Institute for Developmental Disabilities, University of North Carolina at Chapel Hill, Chapel Hill, NC 27599, USA
[4]Department of Psychology, The University of Texas at Austin, Austin, TX 78712, USA
[5]Lead contact
*Correspondence: ddemeter@ucsd.edu
https://doi.org/10.1016/j.celrep.2023.112521

SUMMARY

During childhood, neural systems supporting high-level cognitive processes undergo periods of rapid growth and refinement, which rely on the successful coordination of activation across the brain. Some coordination occurs via cortical hubs—brain regions that coactivate with functional networks other than their own. Adult cortical hubs map into three distinct profiles, but less is known about hub categories during development, when critical improvement in cognition occurs. We identify four distinct hub categories in a large youth sample (n = 567, ages 8.5–17.2), each exhibiting more diverse connectivity profiles than adults. Youth hubs integrating control-sensory processing split into two distinct categories (visual control and auditory/motor control), whereas adult hubs unite under one. This split suggests a need for segregating sensory stimuli while functional networks are experiencing rapid development. Functional coactivation strength for youth control-processing hubs are associated with task performance, suggesting a specialized role in routing sensory information to and from the brain's control system.

INTRODUCTION

Childhood and adolescence mark an extended period of rapid growth and brain development.[1–5] During this time, many neural systems are refined and integrated as children learn and refine complex behaviors. Behavioral successes and delays during development may, at least partially, be associated with individual variations of the normative trajectory of growth and refinement of neural systems throughout the brain. A better understanding of how these systems are organized and interconnected during development may help inform interventions aimed at mitigating delays and supporting successes across different youth populations.

Although the core behaviors that support high-level cognitive control abilities like executive functions (EFs) are established early in life, EF abilities show significant improvement and refinement that continues through young adulthood.[6–8] This period of accelerated learning and behavioral refinement that occurs during childhood coincides with (and is most likely scaffolded by) increased brain maturation and specialization of function that is observed across the cortex.[9–11] Specifically, the successful refinement of neural systems that support behaviors related to EFs such as memory, attention, and cognitive flexibility are increasingly important as children begin to refine the skills that are essential to academic and general life success.[12,13]

Given the complex integration of multiple neural systems that is required for behaviors related to EFs, it is not surprising that EFs appear to recruit and integrate multiple brain regions.[14] Across three EF task domains of working memory, inhibitory control, and cognitive flexibility, cortical regions in the cingulo-opercular, dorsal attention, fronto-parietal, and ventral attention networks, such as the dorsolateral prefrontal cortex (DL-PFC) and the superior parietal cortex, have been identified as key neural substrates of EF task performance.[14–17] Critically, the cortical development that supports high-level cognitive processes such as the updating of working memory, inhibition, and cognitive flexibility is not confined to any one specific brain region.[16,18,19] Further, the developing brain appears to refine and specialize connections between fronto-parietal cortical regions; this refinement of integration between cortical regions may be a key element to increasing "adult-like" performance on EF tasks.[20,21]

The apparent importance of spatially distant cortical regions in the development of EFs during childhood highlights the fact that the association between brain and behavioral development is best characterized using a network view of brain function[22–24] that conceptualizes brain function as coordinated neural activity across many interconnected cortical regions. Using a network view of brain function is key to identifying brain-behavior associations of EFs because it allows for the identification and interpretation of how functional brain networks across the cortex may integrate or connect between one another and how levels of

integration are associated with high-level cognitive processes. This viewpoint then raises two critical questions regarding the integration of cortical regions related to EFs: (1) can common patterns of complex integration of cortical regions be identified during development, and (2) are measures of a higher level of brain network integration associated with a greater ability in high-level cognitive processes?

One method for analyzing the integration of cortical brain regions during childhood is by identifying cortical hubs within resting-state functional coactivation, or "connectivity," (RSFC) data. RSFC data allow us to view brain function as a large, whole-brain network of integrated activity between brain regions that is absent of a specific task state. This whole-brain network of RSFC is then further organized into a set of networks[25–28] that are reliably observed in adult populations. Importantly, activation of cortical regions within these established RSFC networks, such as the cingulo-opercular and fronto-parietal networks, has been shown to be directly related to EF task performance in children.[15] We can quantify between-network integration and the capacity for efficient exchange of information across these brain networks with the identification of nodes that are highly connected to multiple networks. This type of highly connected brain region that connects and integrates functional networks is referred to as a "hub" or "connector hub" region,[29–31] and such hubs have been identified in adults during both rest and active task states.[32–34]

Previous work identifying cortical hubs in adults has not only identified specific cortical regions as connector hubs but has also identified three distinct categories of connector hubs based on functional connectivity profiles of parcels.[35] These categories were named "control-default" (deactivated during all tasks), "cross-control" (deactivated for motor task but activated for memory task), and "control-processing" (activated during all tasks) due to the cortical areas and functional networks they primarily connected. Adult control-default hubs were localized to the dorsal angular gyrus, precuneus, retrosplenial cortex, superior and inferior frontal gyrus, and ventromedial PFC. Adult cross-control hubs, the second hub category, were localized to the inferior parietal lobule, posterior precuneus, middle and superior frontal gyrus, and supramarginal gyrus. Adult control-processing hubs, the final adult hub category, were localized to the dorsomedial PFC, lateral occipital cortex, pre- and postcentral gyrus, and posterior insula. Further, network simulations that removed edges of these hubs from adult whole-brain functional networks resulted in significantly altered brain-wide functional network organization[35] that would result in reduced information flow across the brain. These results suggest that not only are distinct hub types present in the adult functional brain network but that these specific hub regions play a potentially crucial role in the integration and flow of information between functional networks. Cross-control hub regions may play a larger role in tasks that engage higher-level processes, such as those of EF, given their more selective task-related activation in adults.

Given the fact that group-average RSFC networks appear relatively adult-like in childhood[36,37] and that the activation of cortical regions within multiple RSFC networks are associated with EF task performance in childhood,[15] the current study aimed to answer two main questions: (1) are the same three distinct hub categories seen in adults also found in youths (suggesting adult-like functional network integration), or are any of these hub types absent or altered in childhood, and (2) if the integration of multiple networks is necessary for EF task performance, does the functional connectivity strength of identified hubs have practical implications for EFs? Namely, does a higher nodal strength (the average value of all edges connected to that node) of cortical hubs identified in youths relate to better EF task performance? The current study tested the hypothesis that if resting-state cortical hubs can be identified in a youth sample, stronger hubs will reflect better integration of the brain's resting-state functional networks, which will relate to better outcomes on measures of EF task performance.

RESULTS

Cortical hub parcels identified in youths

In order to test for distinct cortical hub categories in our youth sample, we first identified all cortical parcels (predefined brain regions within the Gordon parcellation) that had the network properties of a cortical hub (see STAR Methods: identification of hub parcels). We defined a resting-state cortical hub as any parcel with a participation coefficient value in the top 20% for a given individual. Cortical hub parcels were identified in all 567 participants, and the spatial consistency of hubs was examined across all subjects. While an expected degree of individual variance in hub locations was observed, consistent hub overlap was identified when hub parcels were aggregated across all 567 participants (Figure 1A; right hemisphere images can be found in Figure S1). Hubs were most commonly observed in the bilateral supramarginal gyrus, precuneus, superior parietal lobule, and posterior cingulate; the right superior medial frontal gyrus; and the left inferior temporal gyrus, inferior frontal gyrus, superior frontal gyrus, prefrontal gyrus, and superior parietal lobule (Figure 1B). These peak parcels were members of the cingulo-opercular, cingulo-parietal, fronto-parietal, default mode, dorsal attention, and somatomotor hand resting-state functional networks per the Gordon 333[26] surface parcellation (see Figure 1C for network assignment reference).

Categories of youth cortical hub parcels

After identifying hub parcels across all individuals, we used hub connectivity profiles to then cluster hubs with similar profiles into distinct categories (see STAR Methods: hub parcel categorization). Three sub-groups of participants were created for this hub categorization step (n = 189 participants and 12,633 hub profiles in each group). Across these three sub-groups, either six or seven clusters were identified from the hub profiles within each group (Figure S2). Out of these results, the first four clusters in each group contained enough hub profiles to comfortably be considered hub categories and were assigned a qualitative label. A fifth qualitatively similar cluster was found across the sub-groups (cluster 5 in groups 1 and 2 and cluster 6 in group 3); however, the number of hub profiles in this cluster represented less than 1% of the total. As a result, this cluster was not considered for the main hub categories, nor were the remaining clusters that contained only one or two hub profiles each; these were removed from further analyses.
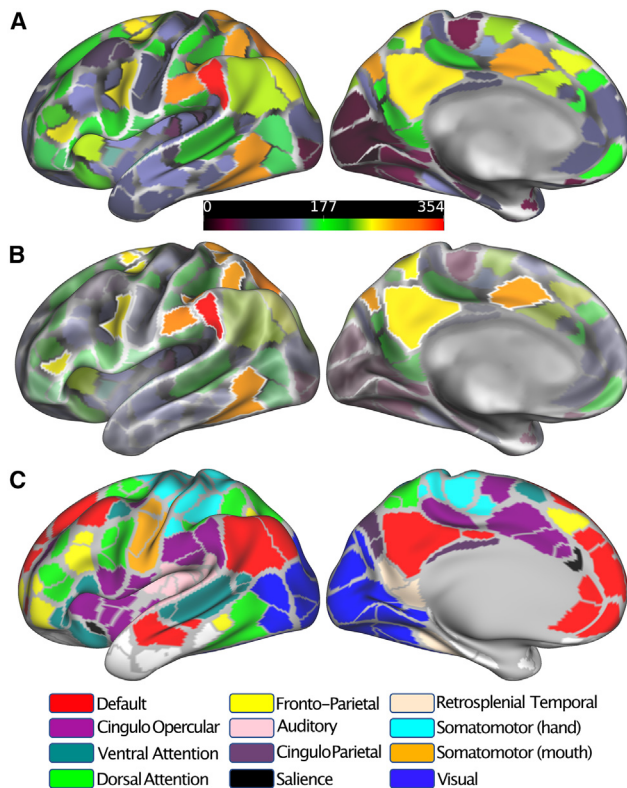
Figure 1. Cortical hub identification

Cortical parcels identified as hubs. All images in are left hemisphere. Right hemisphere images can be found in Figure S1.

(A) Density map of cortical parcels that were labeled as hubs across the full group of 567 participants, illustrating the distribution of hub parcels across the cortex.

(B) Parcels above a 70% threshold on the full group density map (70% chosen only to highlight consistent hubs for visualization purposes) are outlined in white to highlight peak hub regions.

(C) The Gordon 333 parcel set with network assignment key.

Additionally, we checked for any possible influence of participant dataset on each group's identified hub category clusters (i.e., if clusters represented a specific data source, such as the Adolescent Brain Cognitive Development [ABCD] or UT scans, rather than unique hub connectivity profiles). Across all three sub-groups, the identified hub category clusters showed a relatively similar representation of participants from each fMRI collection (Figure S3B, left vertical bar colored by collection). Participants from all datasets showed similar proportions of hubs assigned to each of the four main cluster categories (Figure S3C) across each of the three sub-groups. This suggests that a single hub category was not driven by a specific dataset but rather that all hub categories are present in all included datasets.

The four main clusters were highly similar in all three of our sub-groups (Figure S2) and were then merged across all 567 participants. Hub connectivity profiles for each of these clusters were averaged across all participants, and four final "group-wide" hub categories were created (Figure 2). Hub categories were named based on their connectivity profiles and their resem-

blance to hub categories previously reported in adults.[35] To further confirm the hub category names and groupings, we obtained the hub category density maps from the adult study.[35] The four youth hub category density maps (Figure 2) were correlated with the three adult hub category density maps to quantify their closest adult hub category counterpart (Figure 3A). These comparisons found higher correlations to their counterpart adult hub category density map than 1,000 null models (Figure 3B) created from randomly rotating the youth category density maps on the cortex (see STAR Methods: hub parcel categorization).

The first category (12,983 profiles, 34% of total) contained connections primarily to parcels within the default mode, salience, ventral attention, fronto-parietal, unassigned, and cingulo-parietal networks and was thus named the "youth control-default" hub (Figure 2A). These youth control-default hubs were most similar to the adult control-default category (r = 0.638) and showed peak overlap in parcels located in the bilateral precuneus, supramarginal and angular gyri, middle temporal lobe, and the prefrontal and superior frontal cortex.

The second category of hubs (10,406 profiles, 27.4% of total) contained connections primarily in the dorsal attention, visual, retrosplenial-temporal, somatomotor hand, cingulo-opercular, and cingulo-parietal networks. This second category was named the "youth control-processing (VIS)" (VIS, visual) hub (Figure 2B), was most similar to the adult control-processing category (r = 0.472), and showed peak overlap in parcels located in the inferior temporal lobe, superior parietal cortex, precuneus, superior parietal lobe, and occipital lobe.
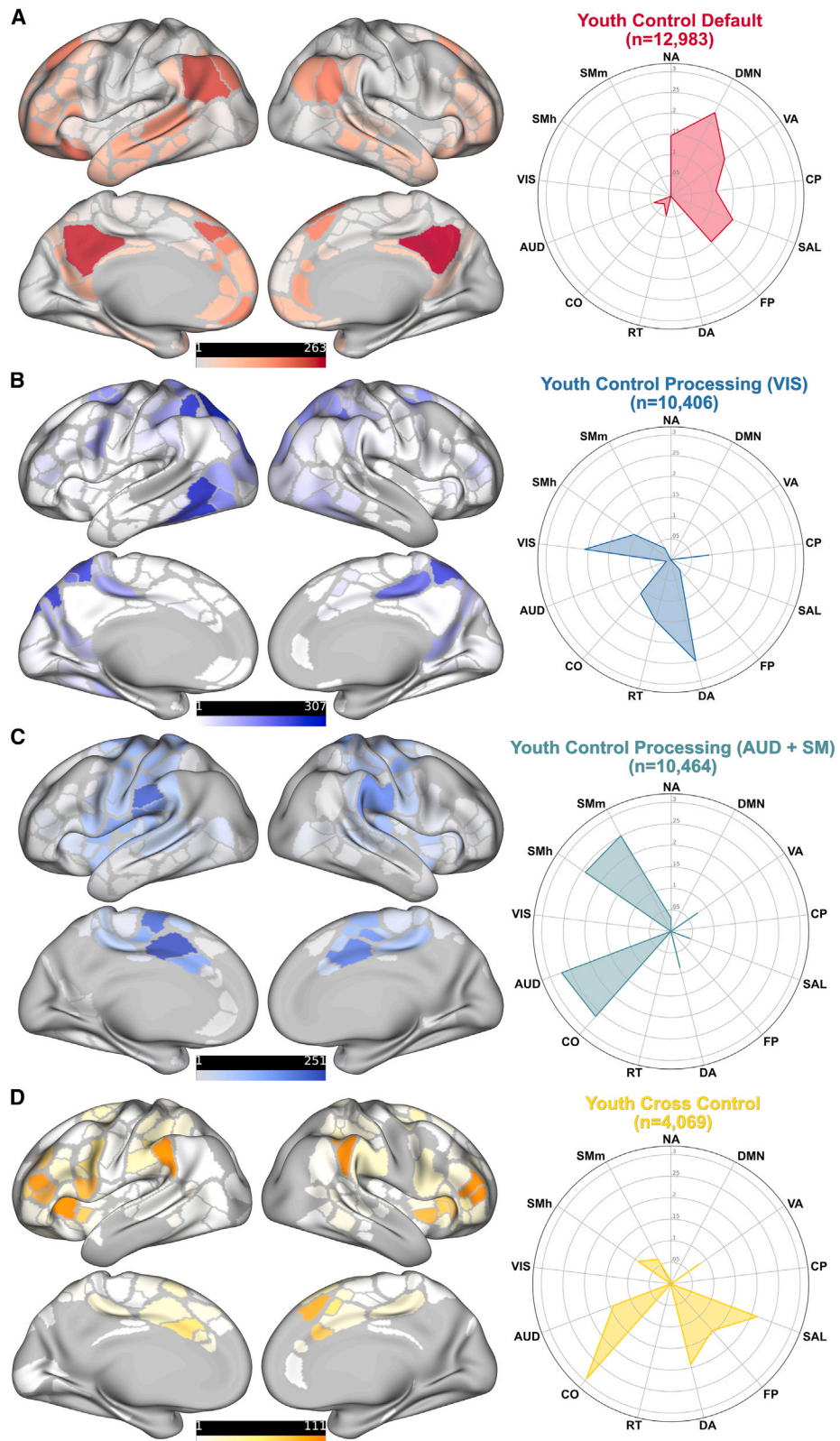
The third category, named the "youth control-processing (AUD + SM)" (AUD, auditory; SM, somatomotor) hub (10,464 profiles, 27.5% of total) was also most similar to the adult control-processing category (r = 0.528), and contained parcels with connections primarily in the auditory, cingulo-opercular, somatomotor mouth, and somatomotor hand functional networks (Figure 2C). These youth control-processing (AUD + SM) hubs showed peak parcel overlap in the supramarginal gyrus, anterior cingulate, posterior insula, and pre- and postcentral gyrus.

The fourth major hub category (4,069 profiles, 10.7% of total) contained parcels with connections primarily in the cingulo-opercular, salience, dorsal attention, fronto-parietal, auditory, and ventral attention networks and was named the "youth cross-control" hub (Figure 2D). Youth cross-control hubs were most similar to the adult cross-control hub category (r = 0.419) and showed peak parcel overlap in the supramarginal gyrus, anterior insula, pars opercularis, middle frontal gyrus, and anterior cingulate.

EF task performance associated with cortical hub connectivity

We tested the role of cortical hubs identified in youths on EF task performance by associating the functional connectivity of hub parcels, within each of the four identified categories, with EF task outcomes. We tested this association by quantifying how hubs may be specialized and support resting-state functional network integration by integrating the functional networks belonging to its assigned hub category. This value represented the average connectivity of all hubs within a given hub category

A Youth Control Default
(n=12,983)

B Youth Control Processing (VIS)
(n=10,406)

C Youth Control Processing (AUD + SM)
(n=10,464)

D Youth Cross Control
(n=4,069)

(legend on next page)

to all parcels within the primary functional networks represented in that given hub category. We labeled this value the "within-hub-category" connectivity. Within-hub-category average connectivity was then correlated with age-corrected scores on the cognitive flexibility and working memory task outcomes from each participant.

The within-hub-category average connectivity for both youth control-processing (VIS) and youth control-processing (AUD + SM) hubs was significantly correlated with the cognitive flexibility task scores ($r = 0.09$, $p = 0.03$ and $r = 0.13$, $p = 0.002$, respectively) before Bonferroni correction for multiple comparisons (Figure 4). However, only the control-processing (AUD + SM) hubs survived Bonferroni correction for eight tests (Bonferroni adjusted p = 0.017). We also reran the same correlation analyses using only the 500 ABCD participants in order to test if the larger range of participant age in the UT sample significantly impacted our outcomes. The results were similar to the whole-group analysis, with both control-processing hubs significantly correlated ($r = 0.10$, $p = .01$ [VIS] and $r = 0.12$, $p = 0.004$ [AUD + SM]) with cognitive flexibility task performance and only the control-processing (AUD + SM) hubs surviving Bonferroni correction (Bonferroni adjusted p = 0.032). Working memory task performance was not significantly associated with any within-hub-category connectivity.

DISCUSSION

Youth control-default and cross-control hubs show more diverse connectivity than in adults

In the current work, we provide evidence that resting-state cortical hub categories resembling those found in adults are established by middle childhood. However, while adult-like cortical hub categories are present in middle childhood, developmental influences on functional network organizational trajectories may explain the inclusion of additional network representation in some youth hub categories. Specifically, we found evidence of ongoing functional network refinement and segregation in our youth control-default and youth cross-control categories (Figures 2A and 2D), evidenced by more diverse functional network representation than that found in their analogous adult hub categories (e.g., the inclusion of stronger connectivity to the salience network and weaker default mode connectivity in youth cross-control hubs, and stronger salience network connectivity in the youth control-default hubs, compared with those observed in adults).

The inclusion of functional networks not found in the adult categories may be due to non-linear developmental trajectories of functional network integration and specialization. Evidence of

this non-linear functional network integration during childhood has been highlighted in previous work[39] and may help explain the more diverse connectivity observed in our youth-specific hub categories. While the current work used participation coefficient (PC) to identify individual parcels exhibiting hub-like connectivity across functional networks, PC has also been used to quantify the overall average integration of resting-state functional networks. Marek and colleagues[39] tracked fluctuations in PC within common resting-state functional networks from early adolescence to young adulthood. From ages 12 to 22, PC values in the default mode network showed a U-shaped trajectory that decreased until around 18 years old and then increased through 22 years old. Alternatively, PC values in the fronto-parietal network increased from 12 to 14 years old, decreased until around 20 years old, and then increased again through 22 years old. These results suggest that, during development, parcels in functional networks fluctuate between connections dominantly within their "home" network to connections dominantly outside of their "home" network.

Although the majority of participants in our sample are younger than the age range in this previous work, their results offer a possible explanation for the increased connectivity profile diversity observed in the youth control-default and cross-control hub categories compared with in adults. For example, during the period of development highlighted in the current work (ages 8–17 years), PC values for parcels within the default mode and fronto-parietal networks for a given individual may rest anywhere upon those non-linear curves. We posit that this fluctuation of PC values during development results in more diverse connectivity patterns for hub categories identified in youths. However, these two hub categories (youth control-default and youth cross-control) were observed across all three of the participant sub-groups (n = 189 each) used for the hub categorization step (Figure S2), suggesting that these youth-specific hub categories are more related to network refinement associated with development than individual differences in our sub-samples of youths.

Two distinct types of youth control-processing hubs
Contrary to the single adult control-processing hub category that integrates sensory networks with the cingulo-opercular and dorsal attention networks,[35] we found that youth control-processing hubs were split into two reliable and distinct categories across subgroups. This evidence of two distinct control-processing hub types in youth (youth control-processing (VIS) and youth control-processing (AUD + SM) hubs; Figures 2B and 2C) may highlight the developmental need for differentiated integration of sensory inputs and outputs to cognitive-control-focused networks. Cortical activation related to cognitive control during task

---

Figure 2. Youth cortical hub categories

(A–D) Four primary cortical hub categories were identified in youths: (1) youth control-default (A) with connectivity primarily in the cingulo-parietal, default mode, fronto-parietal, unassigned, salience, and ventral attention functional networks; (2) youth control-processing (VIS) (B) with connectivity primarily in the cingulo-opercular, cingulo-parietal, dorsal attention, retrosplenial-temporal, somatomotor hand, and visual functional networks; (3) youth control-processing (AUD + SM) (C) with connectivity primarily in the auditory, cingulo-opercular, somatomotor hand, and somatomotor mouth functional networks; and (4) youth cross-control (D) with connectivity primarily in the auditory, cingulo-opercular, dorsal attention, fronto-parietal, salience, and ventral attention functional networks. Heat bars indicate the number of subjects where a given parcel was identified as a hub. AUD, auditory; CO, cingulo-opercular; CP, cingulo-parietal; DMN, default mode; DA, dorsal attention; FP, fronto-parietal; NA, unassigned; RT, restrosplenial-temporal; SAL, salience; SMh, somatomotor hand; SMm, somatomotor mouth; VA, ventral attention; VIS, visual.
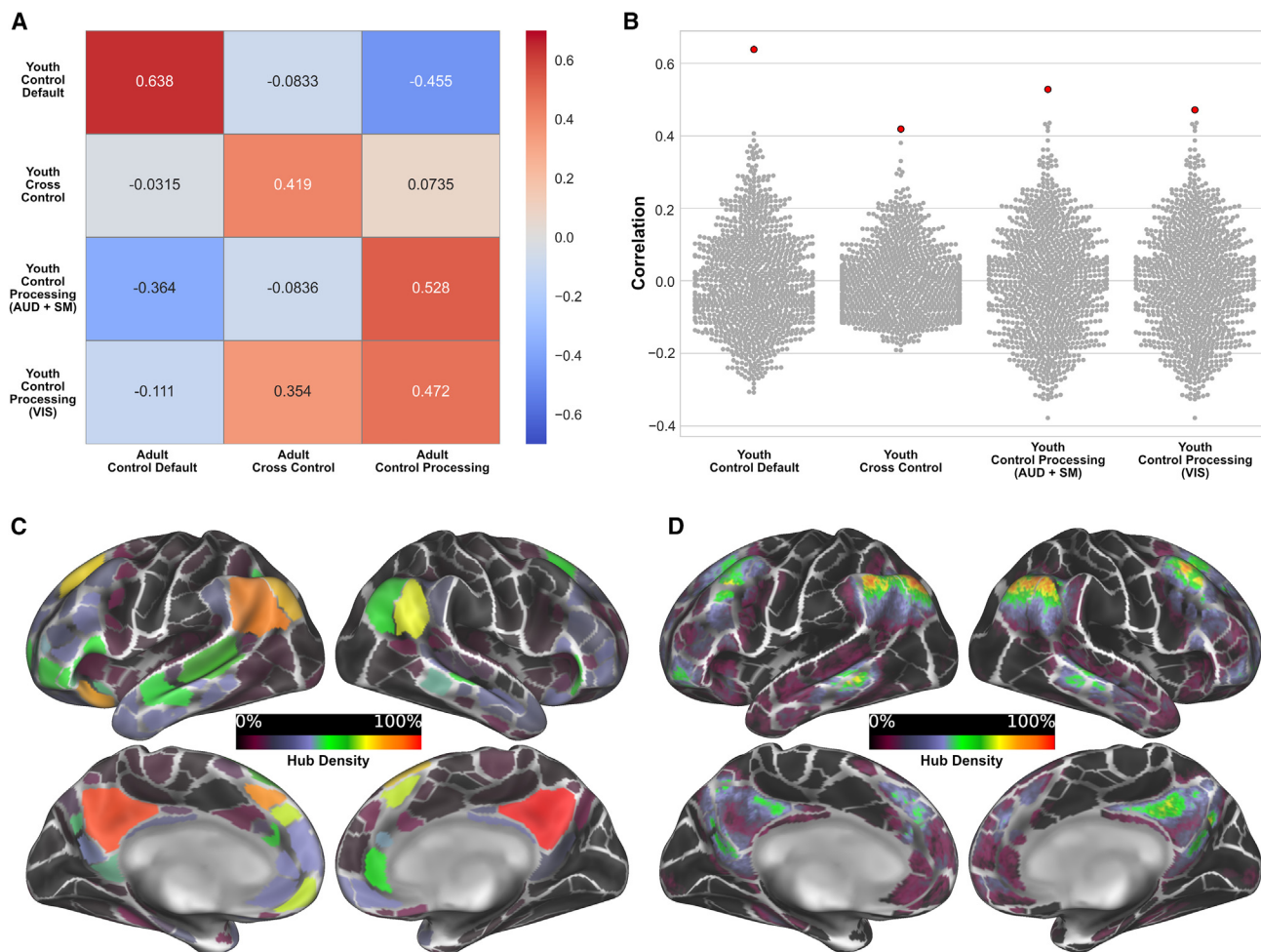
Figure 3. Youth hub density map comparisons with adults
(A) Correlation of youth hub density maps (by hub category) with adult hub density maps obtained from Gordon et al., 2018[35].
(B) Correlations of 1,000 randomly rotated youth hub density maps (by hub category) with the true correlation value highlighted in red.
(C and D) For visualization purposes, an example of the youth control-default hub density map (C) and the parcel-edge censored adult control-default hub density map (D) are provided. Note: prior to correlational comparisons, the youth hub density maps were converted to vertex-wise values.

engagement is anatomically separate from regions directly involved in sensory processing and motor actions, but these regions must coordinate incoming perceptions and outgoing responses for successful task performance.[40] One theory of cognitive control processes outlines a function where cortical regions specialized for control processing may act as intermediaries that route sensory information to and from cognitive-control-specialized networks.[40,41] This proposed system is responsible for processing incoming stimuli, routing this information to networks that make decisions based on that incoming information, and then routing those decisions back to the appropriate outputs for the specific task.

We posit that the control-processing hubs found in youths are differentiated based on sensory input, where the control-processing (VIS) hubs primarily route visual stimuli to the dorsal attention network and the control-processing (AUD + SM) hub primarily routes auditory and somatomotor stimuli to the cingulo-opercular network. The cingulo-opercular and dorsal atten-

tion networks, which are also primary networks within the youth cross-control hubs, then interpret the information and make decisions based on the task, before passing information back to one or both of the control-processing hubs for output. This observed split in control-processing hub categories provides evidence that the functional networks that support this type of cognitive-control-demanding task completion are not yet integrated to the degree seen in an adult sample.[35] We hypothesize that this segregation of sensory stimuli that results in a separation of hub categories in our youth sample is due to the rapid development of cortical regions that belong to the functional networks.

Youth control-processing hubs are related to cognitive flexibility
For the two identified youth control-processing categories (VIS and AUD + SM), we found a significant association (before correction for multiple comparisons) with performance on the
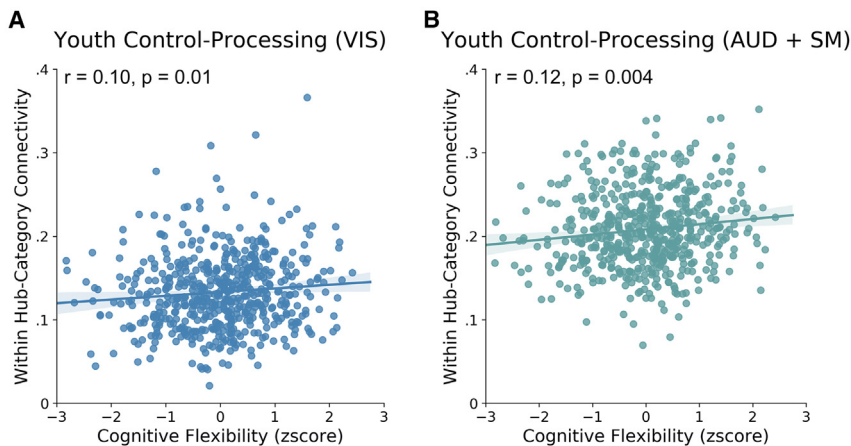
Figure 4. Hub connectivity associated with EF task performance

(A and B) Average within-hub-category connectivity correlated with cognitive flexibility task scores (uncorrected r and p values). Significant associations were observed before Bonferroni correction for the average (A) youth control-processing (VIS) hub connectivity and the average (B) youth control-processing (AUD + SM) hub connectivity. Only the (B) youth control-processing (AUD + SM) results survived Bonferroni correction for 8 tests. Cognitive flexibility scores were age corrected by regressing out the effect of age and then Z scored.

cognitive flexibility task (Figure 4) that was collected out of scanner (see STAR Methods: executive function tasks). Although the control-processing (VIS) results did not survive Bonferroni correction for eight tests, the correlation results follow the same directional trend of the control-processing (AUD + SM) results that did survive correction. We feel that these results are valuable for a better understanding of the association of youth-specific hubs and cognitive flexibility task performance during development. Based on recent work, we expect brain-behavior associations using RSFC data to be very small, even when using very large samples with thousands of participants.[42] The split in the control-processing hub category in youths is the most salient divergence from the adult hub categories, and it is noteworthy that both youth control-processing categories show a similar association with cognitive flexibility task performance. Further investigation is warranted into how these hub categories integrate over age and how this integration may relate to mature EF performance.

Additionally, these results support the theory outlined above that both types of control-processing hubs in youths may act as intermediaries, routing sensory information to and from specialized cognitive-control networks necessary for successful EF task completion. However, given that the network organization tested in this current work is derived from resting-state data, it is impossible to make direct associations in the current work. This hypothesis does, however, align with the theory that connectivity observed in RSFC data represents a long-standing history of coactivation that occurs over the lifetime of an individual.[43–46] We posit that the relationship of youth control-processing hub RSFC with cognitive flexibility task performance is at least partially a result of Hebbian coactivation of these hub regions during development, which is necessary while youths are engaged in the task state.

The association we see in the current study may, in fact, also be highlighting cortical areas previously found to exhibit significant age-related differences in cognitive flexibility tasks.[47] In this previous work, cortical regions within the fronto-parietal, default mode, dorsal attention, and cingulo-opercular functional networks showed significant age effects between adults and youths during the preparatory control period of a similar cognitive flexibility

(switching) task.[47] The regions with the greatest difference between youths and adults during the cue period of the task line up with our youth control-processing (VIS) and control-processing (AUD + SM) categories. In fact, cortical areas in the superior and inferior parietal, inferior temporal, and lateral visual cortex show a large amount of overlap between the peak age differences in that work and our youth control-processing hub peak hub counts. We hypothesize that the similarity of results in these cortical regions may be evidence that youth control-processing hubs are heavily involved in the preparatory control phase of the cognitive flexibility task and are undergoing substantial developmental change in this age range.

Together, these results suggest that individual differences in youth control-processing hub connectivity may impact the successful relay of sensory input to more cognitive-control-specialized networks, like those in the cross-control hub category. During development, this routing of information may be especially important, as these control-processing hubs are not yet consolidated as has been observed in adults.

Limitations of the study

In the current work, we used an established, predefined cortical parcel set[26] to identify cortical hubs in youths. While the use of a predefined parcel set demonstrates the generalizability of hub identification in youths and provides a less computationally intensive method for this work, future work should quantitatively test the difference of hubs defined with preestablished parcels vs. individual-specific parcels (as used in the adult work[35]). Additionally, the current work focuses on a large, cross-sectional sample from three fMRI collections to address the generalizability of hub categories found during development. However, our minimum inclusion criteria for this work was 5 min of postmotion censored data, and previous work has demonstrated that datasets including large quantities of fMRI data (>45 min) result in significant improvements of single-subject RSFC reliability.[48,49] Our future work plans to leverage a highly sampled set of youths with hours of RSFC data, similar to the Midnight Scan Club[50] adult sample, to better investigate individual differences in RSFC hub categories during childhood using precision functional mapping.

To fully understand the development of cortical hub parcels in youths, the developmental trajectory of cortical hubs defined by PC should be carefully considered. It is important that future
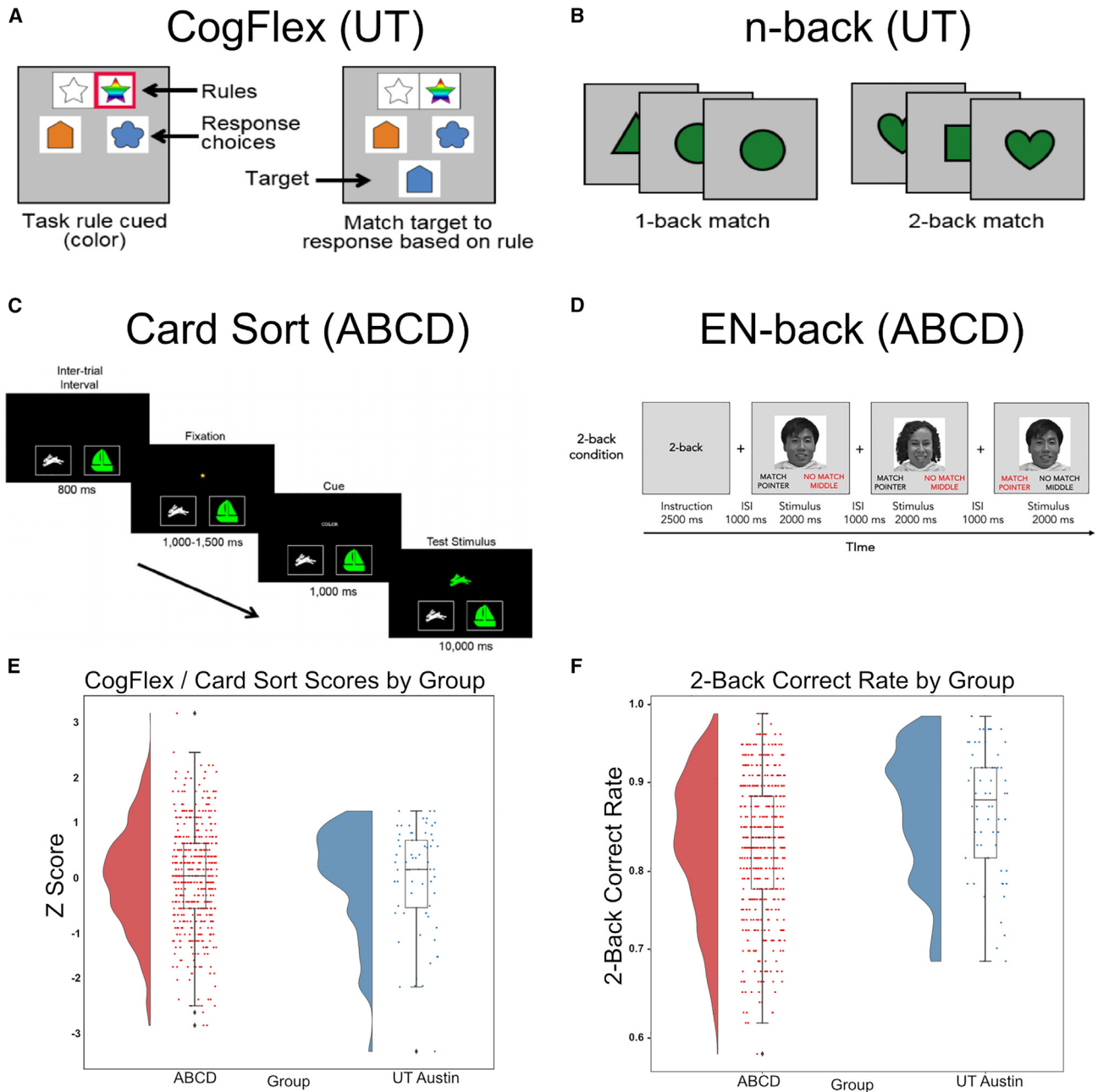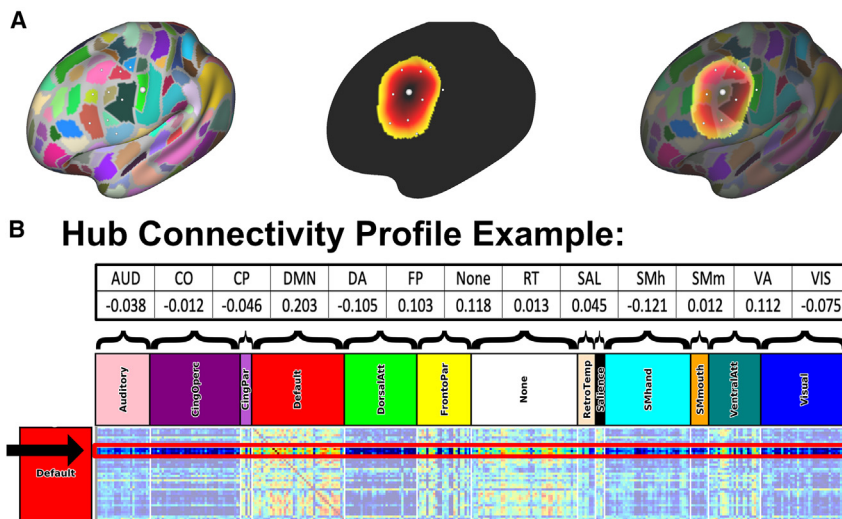
Figure 5. Executive function tasks

(A–F) Examples of the cognitive flexibility tasks administered at the UT site (A, CogFlex) and the ABCD sites (C, dimensional change card sort [image: NIH Toolbox]). Examples of the working memory tasks administered at the UT site (B, n-back) and the ABCD sites (D, emotional n-back [image: Casey et al.[38]]). To match between sites, only trials containing neutral faces and places were used from the emotional n-back (EN-back) (D) task. Task score distributions are also shown, separated by participants group, for the cognitive flexibility (E) and working memory (F) tasks.

work incorporates a longitudinal fMRI dataset that follows individuals from youth to adulthood (e.g., the ABCD study) and tracks how the non-linear change of average PC of functional networks impacts cortical hubs as children age. Of note, many hub regions defined in our youth set belong to resting-state functional networks, such as the default mode and fronto-parietal networks, that have been shown to exhibit vast changes in co-

activation of both within and between network parcels during this period of life.[51–53] Future work should quantify the trajectory of these changes in coactivation and how those changes might influence cortical hub categorization during different periods of development. Such work would add valuable knowledge of how hubs organize longitudinally from youth into adulthood.

A

B

Hub Connectivity Profile Example:

AUD	CO	CP	DMN	DA	FP	None	RT	SAL	SMh	SMm	VA	VIS
-0.038	-0.012	-0.046	0.203	-0.105	0.103	0.118	0.013	0.045	-0.121	0.012	0.112	-0.075

Figure 6. Distance masks and cortical hub profiles

(A and B) Correlations between cortical parcels less than 30 mm geodesic distance of one another were set to zero. This mitigates the impact of spatially close parcels exhibiting higher functional connectivity due to BOLD signal overlap rather than parcel coactivation. One parcel centroid is highlighted (A), and neighboring parcels within and beyond the 30 mm geodesic distance are shown. An example of a hub connectivity profile is illustrated here (B). Profiles are calculated by averaging the connectivity between an identified hub parcel and its connectivity to all parcels within each functional network. This created a profile of 13 values: one average correlation value for each of the predefined functional networks. AUD, auditory; CO, cinguloopercular; CP, cingulo-parietal; DMN, default mode; DA, dorsal attention; FP, fronto-parietal; NA, unassigned; RT, restrosplenial-temporal; SMh, somatomotor hand; SMm, somatomotor mouth; VA, ventral attention; VIS, visual.

Lastly, the brain-behavior associations of cortical hubs to EF task performance that we have highlighted in our youth dataset are specific to functional network organization during resting state. Previous work in adults found that the patterns of functional coactivation or "connectivity" (FC) of connector hubs showed significant changes from rest to task state compared with non-connector hubs.[33] While participants were engaged in tasks, connector hubs showed increased modulation of between-network FC and reduced modulation of within-network FC. Our future work plans to quantify the shift in hub connectivity profiles from resting state to EF task state by replicating these hub identification methods on fMRI data collected while youths were actively engaged in the two EF tasks. We can then test the influence of hub connectivity on task outcomes in these different contexts relative to during rest.

Conclusions

Four main categories of cortical hub parcels, which strongly resemble the three hub categories found in adults, can be iden-tified in their "developmental form" by middle childhood. However, the youth control-processing hubs are split into two distinct categories, and youth control-default and cross-control hub connectivity profiles include more "control" network connections than their similar adult counterparts. Further, FC associated with youth cortical control-processing hub categories showed a distinct relationship with cognitive flexibility task performance. We posit that control-processing hubs act as input/output controllers of sensory information in youths and thus may relate to coordinating and improving complex behaviors in development.

Overall, the results from this work suggest that adult-like cortical hub categories can be clearly identified by middle childhood but that hub category profiles may still be developing, especially in how control networks interface with input and output processors; this developmental configuration may also be influencing performance of some cognitive-control-demanding tasks.

STAR★METHODS

Detailed methods are provided in the online version of this paper and include the following:

- KEY RESOURCES TABLE
- RESOURCE AVAILABILITY
  - Lead contact
  - Materials availability
  - Data and code availability
- EXPERIMENTAL MODEL AND SUBJECT DETAILS
  - Participant demographics
- METHOD DETAILS
  - Executive Function Tasks
  - Cued task switching/cognitive flexibility task
  - Working memory/updating task
  - Neuroimaging acquisition
  - Resting-state preprocessing
- QUANTIFICATION AND STATISTICAL ANALYSIS
  - Identification of hub parcels

Table 1. Participant demographics			
Group demographics			
	UT	ABCD	Combined
Participants	67 (30 F)	500 (254 F)	567 (284 F)
Age range (years)	8.5–17.2	9.0–11	8.5–17.2
Age (mean [M] ± SD)	11.8 ± 2.1	10.1 ± 0.63	10.3 ± 1.1
Mean scan length	9:07	14:30	13:52
Race and ethnicity			
Asian	2	7	9
Black	5	48	53
Hispanic	4	63	67
Multiracial or Other	15	38	53
White	41	344	385

Mean scan length is minutes and seconds of fully preprocessed resting-state scan time, concatenated across all available runs, and postmotion censoring at 0.25 framewise displacement (FD). F, female.

REFERENCES

1. Houston, S.M., Herting, M.M., and Sowell, E.R. (2014). The neurobiology of childhood structural brain development: conception through adulthood. Curr. Top. Behav. Neurosci. *16*, 3–17. https://doi.org/10.1007/7854_2013_265.

2. Barnea-Goraly, N., Menon, V., Eckert, M., Tamm, L., Bammer, R., Karchemskiy, A., Dant, C.C., and Reiss, A.L. (2005). White matter development during childhood and adolescence: a cross-sectional diffusion tensor imaging study. Cerebr. Cortex *15*, 1848–1854. https://doi.org/10.1093/cercor/bhi062.

3. Stiles, J., and Jernigan, T.L. (2010). The basics of brain development. Neuropsychol. Rev. *20*, 327–348. https://doi.org/10.1007/s11065-010-9148-4.

4. Mills, K.L., Goddings, A.-L., Herting, M.M., Meuwese, R., Blakemore, S.-J., Crone, E.A., Dahl, R.E., Güroğlu, B., Raznahan, A., Sowell, E.R., and Tamnes, C.K. (2016). Structural brain development between childhood and adulthood: convergence across four longitudinal samples. Neuroimage *141*, 273–281. https://doi.org/10.1016/j.neuroimage.2016.07.044.

5. Giedd, J.N., Blumenthal, J., Jeffries, N.O., Castellanos, F.X., Liu, H., Zijdenbos, A., Paus, T., Evans, A.C., and Rapoport, J.L. (1999). Brain development during childhood and adolescence: a longitudinal MRI study. Nat. Neurosci. *2*, 861–863. https://doi.org/10.1038/13158.

6. Bauer, J.-R., Martinez, J.E., Roe, M.A., and Church, J.A. (2017). Consistent performance differences between children and adults despite manipulation of cue-target variables. Front. Psychol. *8*, 1304. https://doi.org/10.3389/fpsyg.2017.01304.

7. Best, J.R., and Miller, P.H. (2010). A developmental perspective on executive function. Child Dev. *81*, 1641–1660. https://doi.org/10.1111/j.1467-8624.2010.01499.x.

8. Ferguson, H.J., Brunsdon, V.E.A., and Bradford, E.E.F. (2021). The developmental trajectories of executive function from adolescence to old age. Sci. Rep. *11*, 1382. https://doi.org/10.1038/s41598-020-80866-1.

9. Brown, T.T., and Jernigan, T.L. (2012). Brain development during the preschool years. Neuropsychol. Rev. *22*, 313–333. https://doi.org/10.1007/s11065-012-9214-1.

10. Fair, D.A., Cohen, A.L., Power, J.D., Dosenbach, N.U.F., Church, J.A., Miezin, F.M., Schlaggar, B.L., and Petersen, S.E. (2009). Functional brain networks develop from a "local to distributed" organization. PLoS Comput. Biol. *5*, e1000381. https://doi.org/10.1371/journal.pcbi.1000381.

11. Lenroot, R.K., and Giedd, J.N. (2006). Brain development in children and adolescents: insights from anatomical magnetic resonance imaging. Neurosci. Biobehav. Rev. *30*, 718–729. https://doi.org/10.1016/j.neubiorev.2006.06.001.

12. Best, J.R., Miller, P.H., and Naglieri, J.A. (2011). Relations between executive function and academic achievement from ages 5 to 17 in a large, representative national sample. Learn. Indiv Differ *21*, 327–336. https://doi.org/10.1016/j.lindif.2011.01.007.

13. Jacob, R., and Parkinson, J. (2015). The potential for school-based interventions that target executive function to improve academic achievement. Rev. Educ. Res. *85*, 512–552. https://doi.org/10.3102/0034654314561338.

14. Nowrangi, M.A., Lyketsos, C., Rao, V., and Munro, C.A. (2014). Systematic review of neuroimaging correlates of executive functioning: converging evidence from different clinical populations. J. Neuropsychiatry Clin. Neurosci. *26*, 114–125. https://doi.org/10.1176/appi.neuropsych.12070176.

15. Engelhardt, L.E., Harden, K.P., Tucker-Drob, E.M., and Church, J.A. (2019). The neural architecture of executive functions is established by middle childhood. Neuroimage *185*, 479–489. https://doi.org/10.1016/j.neuroimage.2018.10.024.

16. Fiske, A., and Holmboe, K. (2019). Neural substrates of early executive function development. Dev. Rev. *52*, 42–62. https://doi.org/10.1016/j.dr.2019.100866.

17. Gao, W., Gilmore, J.H., Shen, D., Smith, J.K., Zhu, H., and Lin, W. (2013). The synchronization within and interaction between the default and dorsal attention networks in early infancy. Cerebr. Cortex *23*, 594–603. https://doi.org/10.1093/cercor/bhs043.

18. Dwyer, D.B., Harrison, B.J., Yücel, M., Whittle, S., Zalesky, A., Pantelis, C., Allen, N.B., and Fornito, A. (2014). Large-Scale brain network dynamics supporting adolescent cognitive control. J. Neurosci. *34*, 14096–14107. https://doi.org/10.1523/JNEUROSCI.1634-14.2014.

19. Petersen, S.E., and Sporns, O. (2015). Brain networks and cognitive architectures. Neuron *88*, 207–219. https://doi.org/10.1016/j.neuron.2015.09.027.

20. Buss, A.T., and Spencer, J.P. (2018). Changes in frontal and posterior cortical activity underlie the early emergence of executive function. Dev. Sci. *21*, e12602. https://doi.org/10.1111/desc.12602.

21. Mehnert, J., Akhrif, A., Telkemeyer, S., Rossi, S., Schmitz, C.H., Steinbrink, J., Wartenburger, I., Obrig, H., and Neufang, S. (2013). Developmental changes in brain activation and functional connectivity during response inhibition in the early childhood brain. Brain Dev. *35*, 894–904. https://doi.org/10.1016/j.braindev.2012.11.006.

22. Byrge, L., Sporns, O., and Smith, L.B. (2014). Developmental process emerges from extended brain–body–behavior networks. Trends Cognit. Sci. *18*, 395–403. https://doi.org/10.1016/j.tics.2014.04.010.

23. Mišić, B., and Sporns, O. (2016). From regions to connections and networks: new bridges between brain and behavior. Curr. Opin. Neurobiol. *40*, 1–7. https://doi.org/10.1016/j.conb.2016.05.003.

24. Pessoa, L. (2014). Understanding brain networks and brain organization. Phys. Life Rev. *11*, 400–435. https://doi.org/10.1016/j.plrev.2014.03.005.

25. Doucet, G., Naveau, M., Petit, L., Delcroix, N., Zago, L., Crivello, F., Jobard, G., Tzourio-Mazoyer, N., Mazoyer, B., Mellet, E., and Joliot, M. (2011). Brain activity at rest: a multiscale hierarchical functional organization. J. Neurophysiol. *105*, 2753–2763. https://doi.org/10.1152/jn.00895.2010.

26. Gordon, E.M., Laumann, T.O., Adeyemo, B., Huckins, J.F., Kelley, W.M., and Petersen, S.E. (2016). Generation and evaluation of a cortical area parcellation from resting-state correlations. Cerebr. Cortex *26*, 288–303. https://doi.org/10.1093/cercor/bhu239.

27. Power, J.D., Cohen, A.L., Nelson, S.M., Wig, G.S., Barnes, K.A., Church, J.A., Vogel, A.C., Laumann, T.O., Miezin, F.M., Schlaggar, B.L., and Petersen, S.E. (2011). Functional network organization of the human brain. Neuron *72*, 665–678. https://doi.org/10.1016/j.neuron.2011.09.006.

28. Yeo, B.T.T., Krienen, F.M., Sepulcre, J., Sabuncu, M.R., Lashkari, D., Hollinshead, M., Roffman, J.L., Smoller, J.W., Zöllei, L., Polimeni, J.R., et al. (2011). The organization of the human cerebral cortex estimated by intrinsic functional connectivity. J. Neurophysiol. *106*, 1125–1165. https://doi.org/10.1152/jn.00338.2011.

29. Bertolero, M.A., Yeo, B.T.T., and D'Esposito, M. (2017). The diverse club. Nat. Commun. *8*, 1277. https://doi.org/10.1038/s41467-017-01189-w.

30. Power, J.D., Schlaggar, B.L., Lessov-Schlaggar, C.N., and Petersen, S.E. (2013). Evidence for hubs in human functional brain networks. Neuron *79*, 798–813. https://doi.org/10.1016/j.neuron.2013.07.035.

31. van den Heuvel, M.P., and Sporns, O. (2013). Network hubs in the human brain. Trends Cognit. Sci. *17*, 683–696. https://doi.org/10.1016/j.tics.2013.09.012.

32. Cohen, J.R., and D'Esposito, M. (2016). The segregation and integration of distinct brain networks and their relationship to cognition. J. Neurosci. *36*, 12083–12094. https://doi.org/10.1523/JNEUROSCI.2965-15.2016.

33. Gratton, C., Laumann, T.O., Gordon, E.M., Adeyemo, B., and Petersen, S.E. (2016). Evidence for two independent factors that modify brain networks to meet task goals. Cell Rep. *17*, 1276–1288. https://doi.org/10.1016/j.celrep.2016.10.002.

34. Gratton, C., Sun, H., and Petersen, S.E. (2018). Control networks and hubs. Psychophysiology *55*, e13032. https://doi.org/10.1111/psyp.13032.

35. Gordon, E.M., Lynch, C.J., Gratton, C., Laumann, T.O., Gilmore, A.W., Greene, D.J., Ortega, M., Nguyen, A.L., Schlaggar, B.L., Petersen, S.E., et al. (2018). Three distinct sets of connector hubs integrate human brain function. Cell Rep. *24*, 1687–1695.e4. https://doi.org/10.1016/j.celrep.2018.07.050.

36. Thornburgh, C.L., Narayana, S., Rezaie, R., Bydlinski, B.N., Tylavsky, F.A., Papanicolaou, A.C., Choudhri, A.F., and Völgyi, E. (2017). Concordance of the resting state networks in typically developing, 6-to 7-year-old children and healthy adults. Front. Hum. Neurosci. *11*, 199. https://doi.org/10.3389/fnhum.2017.00199.

37. Grayson, D.S., and Fair, D.A. (2017). Development of large-scale functional networks from birth to adulthood: a guide to the neuroimaging literature. Neuroimage *160*, 15–31. https://doi.org/10.1016/j.neuroimage.2017.01.079.

38. Casey, B.J., Cannonier, T., Conley, M.I., Cohen, A.O., Barch, D.M., Heitzeg, M.M., Soules, M.E., Teslovich, T., Dellarco, D.V., Garavan, H., et al. (2018). The adolescent brain cognitive development (ABCD) study: imaging acquisition across 21 sites. Dev. Cogn. Neurosci. *32*, 43–54. https://doi.org/10.1016/j.dcn.2018.03.001.

39. Marek, S., Hwang, K., Foran, W., Hallquist, M.N., and Luna, B. (2015). The contribution of network organization and integration to the development of cognitive control. PLoS Biol. *13*, e1002328. https://doi.org/10.1371/journal.pbio.1002328.

40. Petersen, S.E., and Posner, M.I. (2012). The attention system of the human brain: 20 Years after. Annu. Rev. Neurosci. *35*, 73–89. https://doi.org/10.1146/annurev-neuro-062111-150525.

41. Power, J.D., and Petersen, S.E. (2013). Control-related systems in the human brain. Curr. Opin. Neurobiol. *23*, 223–228. https://doi.org/10.1016/j.conb.2012.12.009.

42. Marek, S., Tervo-Clemmens, B., Calabro, F.J., Montez, D.F., Kay, B.P., Hatoum, A.S., Donohue, M.R., Foran, W., Miller, R.L., Hendrickson, T.J., et al. (2022). Reproducible brain-wide association studies require thousands of individuals. Nature *603*, 654–660. https://doi.org/10.1038/s41586-022-04492-9.

43. Dosenbach, N.U.F., Fair, D.A., Miezin, F.M., Cohen, A.L., Wenger, K.K., Dosenbach, R.A.T., Fox, M.D., Snyder, A.Z., Vincent, J.L., Raichle, M.E., et al. (2007). Distinct brain networks for adaptive and stable task control in humans. Proc. Natl. Acad. Sci. USA *104*, 11073–11078. https://doi.org/10.1073/pnas.0704320104.

44. Dosenbach, N.U.F., Fair, D.A., Cohen, A.L., Schlaggar, B.L., and Petersen, S.E. (2008). A dual-networks architecture of top-down control. Trends Cognit. Sci. *12*, 99–105. https://doi.org/10.1016/j.tics.2008.01.001.

45. Laumann, T.O., and Snyder, A.Z. (2021). Brain activity is not only for thinking. Curr. Opin. Behav. Sci. *40*, 130–136. https://doi.org/10.1016/j.cobeha.2021.04.002.

46. Newbold, D.J., Gordon, E.M., Laumann, T.O., Seider, N.A., Montez, D.F., Gross, S.J., Zheng, A., Nielsen, A.N., Hoyt, C.R., Hampton, J.M., et al. (2021). Cingulo-opercular control network and disused motor circuits joined in standby mode. Proc. Natl. Acad. Sci. USA *118*, e2019128118. https://doi.org/10.1073/pnas.2019128118.

47. Church, J.A., Bunge, S.A., Petersen, S.E., and Schlaggar, B.L. (2017). Preparatory engagement of cognitive control networks increases late in childhood. Cerebr. Cortex *27*, 2139–2153. https://doi.org/10.1093/cercor/bhw046.

48. Birn, R.M., Molloy, E.K., Patriat, R., Parker, T., Meier, T.B., Kirk, G.R., Nair, V.A., Meyerand, M.E., and Prabhakaran, V. (2013). The effect of scan length on the reliability of resting-state fMRI connectivity estimates. Neuroimage *83*, 550–558. https://doi.org/10.1016/j.neuroimage.2013.05.099.

49. Laumann, T.O., Gordon, E.M., Adeyemo, B., Snyder, A.Z., Joo, S.J., Chen, M.-Y., Gilmore, A.W., McDermott, K.B., Nelson, S.M., Dosenbach, N.U.F., et al. (2015). Functional system and areal organization of a highly sampled individual human brain. Neuron *87*, 657–670. https://doi.org/10.1016/j.neuron.2015.06.037.

50. Gordon, E.M., Laumann, T.O., Gilmore, A.W., Newbold, D.J., Greene, D.J., Berg, J.J., Ortega, M., Hoyt-Drazen, C., Gratton, C., Sun, H., et al. (2017). Precision functional mapping of individual human brains. Neuron *95*, 791–807.e7. https://doi.org/10.1016/j.neuron.2017.07.011.

51. Rubia, K. (2013). Functional brain imaging across development. Eur. Child Adolesc. Psychiatr. *22*, 719–731. https://doi.org/10.1007/s00787-012-0291-8.

52. DeSerisy, M., Ramphal, B., Pagliaccio, D., Raffanello, E., Tau, G., Marsh, R., Posner, J., and Margolis, A.E. (2021). Frontoparietal and default mode network connectivity varies with age and intelligence. Dev. Cogn. Neurosci. *48*, 100928. https://doi.org/10.1016/j.dcn.2021.100928.

53. Sherman, L.E., Rudie, J.D., Pfeifer, J.H., Masten, C.L., McNealy, K., and Dapretto, M. (2014). Development of the default mode and central executive networks across early adolescence: a longitudinal study. Dev. Cogn. Neurosci. *10*, 148–159. https://doi.org/10.1016/j.dcn.2014.08.002.

54. Smith, S.M., Jenkinson, M., Woolrich, M.W., Beckmann, C.F., Behrens, T.E.J., Johansen-Berg, H., Bannister, P.R., De Luca, M., Drobnjak, I., Flitney, D.E., et al. (2004). Advances in functional and structural MR image analysis and implementation as FSL. Neuroimage *23*, S208–S219. https://doi.org/10.1016/j.neuroimage.2004.07.051.

55. Dale, A.M., Fischl, B., and Sereno, M.I. (1999). Cortical surface-based analysis: I. Segmentation and surface reconstruction. Neuroimage *9*, 179–194. https://doi.org/10.1006/nimg.1998.0395.

56. The MathWorks Inc (2020). MATLAB Version: 9.9.0 (2020b). Natick Mass (MathWorks Inc.). www.mathworks.com.

57. Nugiel, T., Roe, M.A., Engelhardt, L.E., Mitchell, M.E., Zheng, A., and Church, J.A. (2020). Pediatric ADHD symptom burden relates to distinct neural activity across executive function domains. Neuroimage. Clin. *28*, 102394. https://doi.org/10.1016/j.nicl.2020.102394.

58. Zelazo, P.D. (2006). The Dimensional Change Card Sort (DCCS): a method of assessing executive function in children. Nat. Protoc. *1*, 297–301. https://doi.org/10.1038/nprot.2006.46.

59. Zelazo, P.D., Anderson, J.E., Richler, J., Wallner-Allen, K., Beaumont, J.L., and Weintraub, S. (2013). II. NIH toolbox cognition battery (CB): measuring executive function and attention. Monogr. Soc. Res. Child Dev. *78*, 16–33. https://doi.org/10.1111/mono.12032.

60. Luciana, M., Bjork, J.M., Nagel, B.J., Barch, D.M., Gonzalez, R., Nixon, S.J., and Banich, M.T. (2018). Adolescent neurocognitive development and impacts of substance use: overview of the adolescent brain cognitive development (ABCD) baseline neurocognition battery. Dev. Cogn. Neurosci. *32*, 67–79. https://doi.org/10.1016/j.dcn.2018.02.006.

61. Jaeggi, S.M., Studer-Luethi, B., Buschkuehl, M., Su, Y.-F., Jonides, J., and Perrig, W.J. (2010). The relationship between n-back performance and matrix reasoning — implications for training and transfer. Intelligence *38*, 625–635. https://doi.org/10.1016/j.intell.2010.09.001.

62. Cohen, A.O., Breiner, K., Steinberg, L., Bonnie, R.J., Scott, E.S., Taylor-Thompson, K.A., Rudolph, M.D., Chein, J., Richeson, J.A., Heller, A.S., et al. (2016). When is an adolescent an adult? Assessing cognitive control in emotional and nonemotional contexts. Psychol. Sci. *27*, 549–562. https://doi.org/10.1177/0956797615627625.

63. Barch, D.M., Burgess, G.C., Harms, M.P., Petersen, S.E., Schlaggar, B.L., Corbetta, M., Glasser, M.F., Curtiss, S., Dixit, S., Feldt, C., et al. (2013). Function in the human connectome: task-fMRI and individual differences in behavior. Neuroimage *80*, 169–189. https://doi.org/10.1016/j.neuroimage.2013.05.033.

64. Peirce, J.W. (2007). PsychoPy—psychophysics software in Python. J. Neurosci. Methods *162*, 8–13. https://doi.org/10.1016/j.jneumeth.2006.11.017.

65. Noble, S., Scheinost, D., Finn, E.S., Shen, X., Papademetris, X., McEwen, S.C., Bearden, C.E., Addington, J., Goodyear, B., Cadenhead, K.S., et al. (2017). Multisite reliability of MR-based functional connectivity. Neuroimage *146*, 959–970. https://doi.org/10.1016/j.neuroimage.2016.10.020.

66. Zhao, N., Yuan, L.-X., Jia, X.-Z., Zhou, X.-F., Deng, X.-P., He, H.-J., Zhong, J., Wang, J., and Zang, Y.-F. (2018). Intra- and inter-scanner reliability of voxel-wise whole-brain analytic metrics for resting state fMRI. Front. Neuroinform. *12*, 54–59. https://doi.org/10.3389/fninf.2018.00054.

67. Marcus, D.S., Harwell, J., Olsen, T., Hodge, M., Glasser, M.F., Prior, F., Jenkinson, M., Laumann, T., Curtiss, S.W., and Van Essen, D.C. (2011). Informatics and data mining tools and strategies for the human connectome Project. Front. Neuroinform. *5*, 4–12. https://doi.org/10.3389/fninf.2011.00004.

68. Glasser, M.F., Sotiropoulos, S.N., Wilson, J.A., Coalson, T.S., Fischl, B., Andersson, J.L., Xu, J., Jbabdi, S., Webster, M., Polimeni, J.R., et al. (2013). The minimal preprocessing pipelines for the Human Connectome Project. Neuroimage *80*, 105–124. https://doi.org/10.1016/j.neuroimage.2013.04.127.

69. Power, J.D., Barnes, K.A., Snyder, A.Z., Schlaggar, B.L., and Petersen, S.E. (2012). Spurious but systematic correlations in functional connectivity MRI networks arise from subject motion. Neuroimage *59*, 2142–2154. https://doi.org/10.1016/j.neuroimage.2011.10.018.

70. Power, J.D., Mitra, A., Laumann, T.O., Snyder, A.Z., Schlaggar, B.L., and Petersen, S.E. (2014). Methods to detect, characterize, and remove motion artifact in resting state fMRI. Neuroimage *84*, 320–341. https://doi.org/10.1016/j.neuroimage.2013.08.048.

71. Hallquist, M.N., Hwang, K., and Luna, B. (2013). The nuisance of nuisance regression: spectral misspecification in a common approach to resting-state fMRI preprocessing reintroduces noise and obscures functional connectivity. Neuroimage *82*, 208–225. https://doi.org/10.1016/j.neuroimage.2013.05.116.

72. Dipasquale, O., Sethi, A., Laganà, M.M., Baglio, F., Baselli, G., Kundu, P., Harrison, N.A., and Cercignani, M. (2017). Comparing resting state fMRI de-noising approaches using multi- and single-echo acquisitions. PLoS One *12*, e0173289. https://doi.org/10.1371/journal.pone.0173289.

73. Caballero-Gaudes, C., and Reynolds, R.C. (2017). Methods for cleaning the BOLD fMRI signal. Neuroimage *154*, 128–149. https://doi.org/10.1016/j.neuroimage.2016.12.018.

74. Lindquist, M.A., Geuter, S., Wager, T.D., and Caffo, B.S. (2019). Modular preprocessing pipelines can reintroduce artifacts into fMRI data. Hum. Brain Mapp. *40*, 2358–2376. https://doi.org/10.1002/hbm.24528.

75. Rosvall, M., and Bergstrom, C.T. (2008). Maps of random walks on complex networks reveal community structure. Proc. Natl. Acad. Sci. USA *105*, 1118–1123. https://doi.org/10.1073/pnas.0706851105.

76. Rubinov, M., and Sporns, O. (2010). Complex network measures of brain connectivity: uses and interpretations. Neuroimage *52*, 1059–1069. https://doi.org/10.1016/j.neuroimage.2009.10.003.

77. Rubinov, M., and Sporns, O. (2011). Weight-conserving characterization of complex functional brain networks. Neuroimage *56*, 2068–2079. https://doi.org/10.1016/j.neuroimage.2011.03.069.

78. Lancichinetti, A., and Fortunato, S. (2012). Consensus clustering in complex networks. Sci. Rep. *2*, 336. https://doi.org/10.1038/srep00336.

Cell Reports
Article

STAR★METHODS

KEY RESOURCES TABLE

REAGENT or RESOURCE	SOURCE	IDENTIFIER
Deposited data		
Adolescent brain cognitive development (ABCD) data	Casey et al.[38]	RRID:SCR_015769 https://nda.nih.gov/abcd
Software and algorithms		
FMRIB Software Library (FSL)	Smith et al.[54]	RRID:SCR_002823; https://fsl.fmrib.ox.ac.uk/fsl/fslwiki
Freesurfer	Dale et al.[55]	RRID:SCR_001847; https://surfer.nmr.mgh.harvard.edu/
MATLAB	Mathworks[56]	RRID:SCR_001622; https://www.mathworks.com/
Original Code for this Manuscript	This paper	https://doi.org/10.5281/zenodo.7814714

RESOURCE AVAILABILITY

Lead contact
Correspondence and requests for materials should be addressed to Damion V. Demeter (ddemeter@ucsd.edu).

Materials availability
This study did not use or generate new unique reagents.

Data and code availability
- Data used in the preparation of this article were obtained from the Adolescent Brain Cognitive Development (ABCD) Study (https://abcdstudy.org). ABCD consortium investigators designed and implemented the study and/or provided data but did not participate in the analysis or writing of this report. This manuscript reflects the views of the authors and may not reflect the opinions or views of the NIH or ABCD consortium investigators. The ABCD data repository grows and changes over time. The ABCD data used in the analyses of this report can be found under the NDA Study DOI: 10.15154/1522676. DOIs can be found at https://nda.nih.gov/general-query.html.
- Original code used in this work to identify and categorize cortical hubs can be found on the main author's github page https://github.com/iamdamion (https://doi.org/10.5281/zenodo.7814714).
- Additional information is available from the lead contact upon request.

EXPERIMENTAL MODEL AND SUBJECT DETAILS

Participant demographics
Participants in this combined dataset (Table 1) of 567 (284 F) youths were recruited either at the University of Texas at Austin (UT) (n = 67) or as part of the publicly available Adolescent Brain Cognitive Development (ABCD) study (n = 500). All participants included in this study were required to have at least 5-min of post-processed resting state scan data, after motion censoring using a .25 framewise displacement (FD) threshold (see post-motion censored time distribution in supplement (Figure S3A)). Participants from the UT dataset were recruited for either a longitudinal, multidimensional study of executive function (e.g., Nugiel et al.[57]), or as part of the Texas Twin Project.[15] This combined dataset is comprised of youths ages 8.5–17.2 (M = 10.3) years-old at the time of scan, and only one twin sibling (pseudo-randomly selected) was included from any family pair to minimize the influence of genetic similarity on our results. The UT sample included 3 participants that had ever received an ADHD diagnosis and the ABCD sample included 77 participants that had ever been diagnosed with ADHD, depression, bipolar disorder, anxiety, or a phobia, per parent report. Exclusion criteria for these datasets included a reported history of epilepsy, head trauma, or any non-removable metal implant that would prevent participation in the MRI portion of the study.

Institutional review board (IRB) approval was received from the University of Texas at Austin (IRB #2014-09-0116; IRB #2016-06-0025) and from the respective IRB sites associated with the Adolescent Brain Cognitive Development collection (DAR ID 11833). Written assent was obtained by participants and written informed consent was obtained by their caregivers.

METHOD DETAILS

Executive Function Tasks

The current study focused on tasks designed to target cognitive flexibility and working memory/updating EF abilities. Tasks were matched as closely as possible between the University of Texas at Austin (UT) and the ABCD dataset, although slight differences in the presented tasks are noted in the task details section. Further, in an effort to mitigate the influence of setting (tasks completed inside or outside of MRI scanner) on task performance, task setting was matched between the two datasets. Therefore, the cognitive flexibility task scores were collected from tasks performed outside of the scanner, while the working memory/updating task was performed within the scanner. Similarly, we either normalized or matched the task scoring method reported for the ABCD dataset to mitigate differences between reported scores within the two datasets (see Figures 5E and 5F for distribution of task scores across collections).

Cued task switching/cognitive flexibility task

Participants in the UT dataset completed 46 trials of a cued rule matching task aimed to assess cognitive flexibility[15,47] while outside of the scanner (Figure 5A). For each trial, participants were cued to match a target stimulus based on one of two possible rules (match the shape or color). Response choices were displayed for the duration of the trial. For the first 1.5 s of each trial a red box would indicate the rule to follow. The target stimulus then appeared .5 s after the red box indicating the rule had disappeared and the stimulus remained on screen for 2 s. During this time, the participant would indicate which response choice matched the target, according to the rule. After each response period, a fixation cross was displayed for 1–4 s. All participants completed a brief practice example set to confirm they understood the task. Z-scores calculated from task accuracy scores (correct/total trials) were used for our analyses.

Participants in the ABCD dataset completed a similar switching task from the NIH Toolbox Cognition Battery; the Dimensional Change Card Sort (DCCS) test[58–60] while outside of the scanner (Figure 5C). During the DCCS, participants are presented with two objects at the bottom of the screen. A third object is then presented in the middle of the screen and the participant is asked to match it to one of the two objects on the bottom of the screen, either by shape or color. All participants are first given a practice set, followed by a block of trials where they match based on one rule, a block where they match on the other rule, and then a block where the rule is pseudo-randomly alternated between the shape and color rules. The DCCS provides a standard score metric (normative mean = 100, SD = 15) that is not age corrected, and is provided to gauge a participant's overall level of functioning on the task. This score was then converted to z-scores for appropriate use with the UT dataset. This non-age-corrected score was used as age correction is done later in our analyses.

Working memory/updating task

Participants in the UT dataset completed up to two versions of a block design, n-back task[15] while inside the scanner (Figure 5B). At the start of each scan, the participants were verbally reminded of the rules of the task by the scan operator. The n-back task was adapted from[61] and is used to assess an individual's working memory or updating ability. Each task run consisted of 64 shape stimuli in a fixed block design that were evenly divided into a 1-back and 2-back block. At the start of each block, participants were shown instructions for 4 s that indicated if they should look for shapes shown one shape prior (1-back) or two shapes prior (2-back). Each stimulus was shown for 1.5 s with a 1 s inter-stimulus interval. Participants were instructed to push a button when they believed the shape they were currently viewing matched a shape either one or two shapes previous, based on the instructions. Each block was followed by a 20 s fixation cross, and a total of 7 matches were shown in each block (21.0% of trials). The correct rate was calculated (total correct/total stimuli shown) for only the 2-back trials, and this measure of task performance was used in our analyses.

Participants in the ABCD dataset completed up to two runs of an emotional n-back (EN-back) (Figure 5D) task while in the scanner.[38,62,63] The EN-back task is a variant of the Human Connectome Project n-back task[63] and measures working memory processes. The task includes two runs of eight blocks where participants are asked to indicate if an image matches or does not match based on a 0-back or a 2-back rule. In the EN-back, trials consist of both emotional faces (such as happy or fearful) and neutral faces or places. During the 2-back section participants are asked to indicate ''match'' when the current stimulus matches a target presented two trials back. Each block consists of 10 trials displayed for 2.5 s each and 4 fixation blocks displayed for 15 s each. Each stimulus was presented for 2 s followed by a 500ms fixation cross. During each block, two of the trials are targets, 2–3 are non-target lures, and the remaining trials are non-lures. To match the UT dataset, our analyses only included task performance on the 2-back, non-emotional segments of the task, which was 4 blocks. We then calculated the correct rate (matching the UT dataset task performance measure) and this measure was used for our analyses.

Neuroimaging acquisition
The university of Texas at austin

All participants scanned at the University of Texas at Austin (UT) were scanned in the Biomedical Imaging Center on a Siemens Skyra 3 T scanner, with a 32-channel head coil. Foam padding was used around the head for comfort and to reduce head motion, and verbal feedback on body motion and to ensure participant comfort was provided between scans. One T1-weighted structural MPRAGE sequence (TR = 2530ms, TE = 3.37ms, FOV = 256x256, voxel resolution = 1 × 1 × 1mm) scan and one T2-weighted structural image

using a turbo spin echo sequence (TR = 3200ms, TE = 412ms, FOV = 256x256, voxel resolution = 1 × 1 × 1mm) were collected and included in the preprocessing steps for this study.

Up to two, 6-min echo-planar sequence functional resting-state scans (TR = 2000ms, TE = 30ms, flip angle = 60°, MB factor = 2, 48 axial slices, voxel resolution = 2 × 2 × 2mm) were collected. All resting-state scans were acquired with the participant instructed to view a white fixation cross on a black background. Participants were instructed to simply stay awake and lie still. Up to two working memory task functional scans were collected (see n-back description above) using the same acquisition settings reported for the resting-state scans. All tasks were run using PsychoPy version 1.8[64] with stimuli projected behind the scanner that participants viewed using a mirror attached to the head coil. Participants recorded their responses during this task using a two-button response pad.

Adolescent brain cognitive development (ABCD) study

In an effort to avoid any unknown scanner manufacturer confounds,[65,66] only participant scans collected on a 3T Siemens Prisma scanner were included in this dataset. All ABCD participant scans were downloaded in their unprocessed form from the NIH Data archive (https://nda.nih.gov/abcd) and preprocessed using our in-house preprocessing pipeline. One T1-weighted structural scan (TR = 2500ms, TE = 2.88ms, FOV = 256x256, voxel resolution = 1 × 1 × 1mm) and one T2-weighted structural scan (TR = 3200ms, TE = 565ms, FOV = 256x256, voxel resolution = 1 × 1 × 1mm) were used for our pre-processing. Up to four, 5-min resting-state scans (TR = 800ms, TE = 30ms, flip angle = 52°, MB factor = 6, 60 axial slices, voxel resolution = 2.4 × 2.4 × 2.4mm) and up to two working memory functional scans (see EN-back description above) were collected and used in this study. For complete information on the ABCD scan protocol, see Casey et al.[38]

Resting-state preprocessing

In-house preprocessing pipeline

To mitigate confounds to analyses that stem from preprocessing decisions, all participants' scans were preprocessed using our in-house pipeline comprised of FMRIB Software Library,[54] Freesurfer,[55] and Connectome Workbench[67] commands, along with custom MATLAB[56] computational scripts. The pipeline follows the first three steps of the Human Connectome minimal preprocessing pipeline,[68] followed by volume and surface preprocessing steps developed in-house, informed by current best practices for resting-state analyses.[69–74]

Volume resting-state preprocessing steps included: (1) motion correction and registration to 2mm MNI atlas space; (2) mode 1k normalization; (3) temporal band-pass filtering (0.009Hz < f < 0.08 Hz); (4) demeaning and detrending of fMRI data; and (5) regression of band-pass filtered nuisance signals including six directions of motion plus their derivatives, cerebral spinal fluid, white matter, and whole brain signal. To reduce the reintroduction of noise that occurs with multiple transformations, all registration steps were done in one single transform. Similarly, all nuisance signal regression and temporal filtering was performed simultaneously.[74]

Surface resting-state preprocessing steps work on the unsmoothed, but fully preprocessed volume scans from the volume pre-processing stage and maps those outputs to 32k fs_LR surface space using the following steps: (1) creation of gray matter ribbon using the white and pial boundaries previously created during the HCP steps; (2) downsampling of gray matter ribbon to functional scan dimensions; (3) exclusion of voxels with high coefficient of variation to improve SNR (following the HCP pipeline's "fMRISurface" procedure); (4) mapping of volume functional data to 32k fs_LR surface mesh; (5) spatial smoothing (2mm FWHM); (6) and creation of CIFTI dense timeseries file.

QUANTIFICATION AND STATISTICAL ANALYSIS

Identification of hub parcels

Identification and categorical labeling of cortical hub nodes (parcels) largely followed the methods outlined by Gordon and colleagues using an adult sample.[35] We identified hub nodes by first extracting resting-state timeseries for each individual, using a predefined cortical surface parcellation set[26] consisting of 333 unique parcels. Values for all vertices within each parcel were averaged and then cross-correlated to create a 333x333 connectivity matrix, which was then Fisher-transformed. The spatial relationship of parcels was taken into consideration by setting correlations of parcels that are within 30mm geodesic distance of one another to zero to mitigate the impact of BOLD signal overlap on between-parcel coactivation (Figure 6A). Next, community detection was applied to each individual's matrix using the Infomap algorithm[75] across a set of edge density thresholds ranging from 0.3% to 5%. At each density threshold, the Infomap algorithm was run using a random seed and 1k iterations. This method provided individually-specific community labels, for all parcels, at each matrix density threshold.

The participation coefficient (PC) metric was then calculated for each parcel, across all density thresholds, using the previously defined individually-specific community labels provided by Infomap. PC for any parcel with a degree (the number of connections to other parcels in the network) in the bottom 25th percentile of all parcels was set to zero. This degree censoring step is performed due to parcels with a low degree providing unstable or inflated PC values.[35] Finally, PC values were then converted to percentiles. This percentile value, averaged across all thresholds, was used for hub identification. For our analyses, the top 20% of parcels for a given individual (calculated from the percentile values of the previous step) was labeled as a hub; following the threshold suggested

by Gordon and colleagues. While there is no established cutoff for labeling a parcel a hub vs. a non-hub, nearly identical results were found using cutoffs from the 75th to 95th percentile[35] and the 80th percentile cutoff is also reported in the previous adult work. Using the 80th percentile cutoff resulted in 67 hubs for each participant.

Hub parcel categorization

Following hub identification, a connectivity profile was calculated for each hub. Hub connectivity profiles are created by calculating the functional connectivity strength between each hub and all other parcels (excluding the hub's self-correlation). Connectivity strengths are then averaged across all within-network parcels to create a connectivity profile consisting of 13 averaged connectivity strengths (one for each of the 13 independent networks in the Gordon parcellation) for each hub (Figure 6B).

Once hub connectivity profiles were created for all identified hubs, hub category types were assigned by clustering together hubs that displayed a similar connectivity profile. We pseudo-randomly split our main sample into three groups of 189 participants (with equal representation from the UT and ABCD datasets) to assess the stability of clusters found within our dataset. For each of these three groups of 189 participants, the following steps were completed: (1) First, we cross-correlated all identified hubs for all 189 group participants to create a correlation matrix of hub profiles (12,663 x 12,663 matrix). (2) This correlation matrix was then used to identify clusters within the set of hub profiles using the Louvain algorithm function[76] from the brain connectivity toolbox. The Louvain algorithm was applied to this signed matrix 1,000 times, using the asymmetric negative weight argument which preserves, but down-weights negative connections as suggested for functional brain networks.[77] (3) An "association-recluster" strategy (also referred to as consensus clustering) was used to address the concern that modularity-based clustering is often non-deterministic, and each iteration can result in different community assignments, despite the same input matrix. A consensus clustering assignment was created by calculating the frequency, across the 1,000 Louvain iterations, that nodes co-occurred in the same community.[78] (4) This final consensus community assignment vector was used to group together hubs with similar connectivity profiles, and categorize each group based on the average connectivity profile of all cortical hubs clustered into that group. (5) Each of these cluster groups were then qualitatively compared to the three cortical hub categories described in the adult literature.[35] Hub category names were then assigned to each cluster group based on the average connectivity profile for all hubs in that group.

To test the appropriateness of our youth hub category names, the three adult hub category density maps were obtained from the authors of the previous adult literature,[35] and additional comparisons to the adult hub density maps were conducted. First, youth hub density maps for each category were correlated against their adult counterparts (Figure 3A). For this step, values in regions between cortical parcels in the adult maps were masked out and comparisons were conducted vertex-wise (see Figure 3D for visualization of masked adult control-default density map). Comparisons of the adult hub density maps to null models of the youth hub density maps were then conducted to highlight the true correlational relationship of the youth maps to the adult maps (Figure 3B). The null models were created by randomly rotating all cortical parcels within the youth hub category density maps using a random cortical rotations method.[26] In this random cortical rotations method, 1K density maps are created by randomly placing parcels of the same size and shape around the cortex, while maintaining the parcels relative position to one another. This method creates a null model that is then appropriate for comparisons between the true youth and adult hub category density maps.

Cortical hub brain-behavior analyses

After hub categories were assigned for all cortical hubs, we then assessed the relationship of resting-state functional connectivity (RSFC) of cortical hub types with EF task performance. First, the "within hub-category" average connectivity was calculated for all cortical hubs within each category, for all participants. This value was calculated using only connectivity from each hub to parcels within the main functional networks represented in the hub category of interest. This provided one average connectivity value for each participant that represented the average connectivity of parcels within the main functional networks of a given hub category, to all hubs belonging to that hub category. The average "within hub-category" connectivity values were then correlated with both the cognitive flexibility and working memory task performance measures. For all tests, the cognitive flexibility and working memory task scores were corrected for participant age via regression, and significance values were Bonferroni corrected for multiple comparisons (eight tests).